IEEE Access
Multidisciplinary | Rapid Review | Open Access Journal

Date of publication xxxx 00, 0000, date of current version xxxx 00, 0000.

Digital Object Identifier 10.1109/ACCESS.2022.Doi Number

Initialization of SINS/GNSS Error Covariance Matrix Based on Error States Correlation

Jun Tang[1,2], Hongwei Bian[1], Heng Ma[1] and Rongying Wang[1]

[1]Department of Navigation Engineering, Naval University of Engineering, Wuhan, CO 430033, China
[2]Department of Navigation, Dalian Naval Academy, Dalian, CO 116018, China

Corresponding author: Hongwei Bian (bhwdegree@163.com).

This work was supported in part by National Natural Science Foundation of China under Grant 41876222.

ABSTRACT The traditional Strapdown Inertial Navigation System (SINS)/Global Navigation Satellite System (GNSS) integrated system uses standard Kalman Filter (KF) to estimate the error states, which weakens the correlation between the different error components to directly initialed the Error Covariance Matrix (ECM) into diagonalization. This initialed method is also widely applied in State Transformation Extended Kalman Filter (STEKF) and Invariant Extended Kalman Filter (IEKF), which results in state estimation failing to achieve the optimal performance. To solve this problem, this paper first analyses the transformed relationship from traditional linear error state to the nonlinear error state redefined in STEKF and IEKF, and the strong correlation is found between the redefined error state components, namely the ECM in STEKF or IEKF no longer appears as a diagonal matrix. Then, aiming at the nonlinear error states, the transformed models of ECM in STEKF and IEKF are derived respectively, which establishes the theoretical basis for ECM initialization based on the error states correlation. Finally, the accuracy, feasibility and general applicability of the proposed method are verified by a boat-mounted field trial.

INDEX TERMS correlation, error covariance matrix, IEKF, SINS/GNSS, STEKF

I. INTRODUCTION

The SINS/GNSS integrated system can give full play to the advantages of SINS and GNSS to make up for the disadvantages of each other, which has been widely used in remote sensing measurement and navigation of various platforms [1,2]. The traditional error state model of SINS/GNSS is established with linear approximation, and KF is usually adopted for states estimation, which could meet the application requirements under general conditions [3,4]. However, in some special and complex situations, such as initial information loss or unreliability, prior information interruption or interference, the reliability of traditional SINS/GNSS will decline significantly [5-8]. In order to solve this problem, STEKF and IEKF have been widely concerned by scholars in recent years. STEKF takes into account the deviation between the calculated navigation frame and the factual navigation frame caused by attitude error (i.e. misalignment angle), and redefines the nonlinear velocity error state [9]. Compared with the traditional filtering algorithms, STEKF has better estimation performance, especially in the case of large misalignment angle [10,11]. IEKF defines a nonlinear error state model based on Lie group, which has the characteristic of autonomous estimation. This means that the error state propagation obeys the linear differential equation, which is independent of the nonlinear change of navigation state [12,13]. Currently IEKF has been used in a variety of integrated navigation systems [7,8,16,17]. The essence of the above two filtering algorithms used in SINS/GNSS can be understood as redefining the nonlinear error state which satisfies the linear differential equation to solve the linearization error problem in traditional SINS/GNSS based on KF [18,19]. However, the initialization of ECM corresponding to the transformed error state has not attracted enough attention.

ECM is defined as the mathematical expectation of the deviation between the state estimation and the true value. The diagonal element of ECM is the variance of each state component estimation, and its square root represents the uncertainty of the state estimation. The non-diagonal element is the covariance reflecting the correlation between the estimation errors of different state components [20]. Proper ECM initialization method can

directly improve the effect of system states estimation. The error states of SINS/GNSS based on KF is linear, which can be considered that there is no correlation or weak correlation among the initial estimated errors, so the ECM can usually be initialized into a diagonal matrix. At present, there are two main ECM initialization methods for STEKF and IEKF. One is directly to calculate the initial variance of each state component according to the traditional error states, and then to set ECM as a diagonal matrix. The other is first to convert traditional error states to the new error states defined by STEKF or IEKF, and then to calculate the initial variance of each new state component, finally to set ECM as a diagonal matrix [9,21]. However, the former is only applicable to the case of small initial misalignment angle and low velocity. Although the latter has better applicability, the convergence speed and accuracy of error state still have further optimization space. In fact, both STEKF and IEKF redefined the nonlinear error states, and there was a strong correlation between the error state components. It was obviously unreasonable to roughly initialize ECM into a diagonal matrix. According to the above analysis, the ECM initialization method is proposed based on the correlation of nonlinear error states. The main innovative contributions of this paper are summarized as follows.

a. The theoretical basis of traditional ECM initialization was analyzed based on the models derivation.

b. The conversion model of ECM for SINS/GNSS based on STEKF is deduced and verified by experiment.

c. The conversion model of ECM for SINS/GNSS based on IEKF is deduced and verified by experiment.

d. The ECM initialization method proposed in this paper is not only applicable to SINS/GNSS, but also has excellent performance in SINS/DVL (Doppler Velocity Log) [22,23], SINS/CNS (Celestial Navigation System) [24,25] and other integrated system.

e. The ECM initialization based on error states correlation is not only suitable for STEKF and IEKF, but also can be used in other optimal estimation algorithms with transformed states.

This paper is organized as follows. Sections II presented the derivation process of the ECM for SINS/GNSS based on KF. The conversion models of ECM for SINS/GNSS based on STEKF and IEKF were respectively deduced in section III and section IV. A boat-mounted field trial was conducted to verify the proposed method in section V. Section VI summarizes the whole paper and puts forward the application prospect.

II. ECM OF SINS/GNSS BASED ON KF

The attitude, velocity and position (avp) error states of SINS/GNSS based on KF could be defined as $\boldsymbol{X}_n = [(\boldsymbol{\phi}^n)^T \ (\delta\boldsymbol{v}^n)^T \ (\delta\boldsymbol{p}^n)^T]^T$, which is represented in East-North-Up (ENU) local navigation frame. The estimation of $\boldsymbol{X}_n$ is described as $\tilde{\boldsymbol{X}}_n = [(\tilde{\boldsymbol{\phi}}^n)^T \ (\delta\tilde{\boldsymbol{v}}^n)^T \ (\delta\tilde{\boldsymbol{p}}^n)^T]^T$, where $\tilde{\bullet}$ serves as the estimated value. When the initial error state estimation $\tilde{\boldsymbol{X}}_n(0)$ is a zero vector, the ECM can be expressed as

$$\boldsymbol{P}_n = \mathrm{E}(\boldsymbol{X}_n\boldsymbol{X}_n^T) = \begin{bmatrix} \mathrm{E}[(X_n^1)^2] & \mathrm{E}[X_n^1X_n^2] & \cdots & \mathrm{E}[X_n^1X_n^9] \\ \mathrm{E}[X_n^2X_n^1] & \mathrm{E}[(X_n^2)^2] & \cdots & \mathrm{E}[X_n^2X_n^9] \\ \vdots & \vdots & & \vdots \\ \mathrm{E}[X_n^9X_n^1] & \mathrm{E}[X_n^9X_n^2] & \cdots & \mathrm{E}[(X_n^9)^2] \end{bmatrix} \tag{1}$$

Where $\mathrm{E}(\bullet)$ is Mathematical expectation operator. $X_n^i \ (i = 1, 2\cdots, 9)$ is the component of $\boldsymbol{X}_n$. The diagonal element of $\boldsymbol{P}_n$ is the variance of avp error state component, and its square root represents the uncertainty of the error state estimation. The non-diagonal element is the covariance reflecting the correlation between the estimation errors of different state components. When ECM is initialized, it can be roughly considered that the initial estimates of different error state components are not correlated, that is, the covariance is satisfied

$$\mathrm{E}[X_n^iX_n^j] = 0 \ (i \neq j) \tag{2}$$

Therefore, (1) can be converted to

$$\boldsymbol{P}_n = diag(\mathrm{E}[(\tilde{X}_n^1)^2] \ \mathrm{E}[(\tilde{X}_n^2)^2] \ \cdots \ \mathrm{E}[(\tilde{X}_n^9)^2]) \tag{3}$$

Where $diag(\bullet)$ is the diagonal matrix operator. Let

$$\boldsymbol{P}_n = \begin{bmatrix} \boldsymbol{P}_{\phi^n} & 0_{3\times3} & 0_{3\times3} \\ 0_{3\times3} & \boldsymbol{P}_{\delta v^n} & 0_{3\times3} \\ 0_{3\times3} & 0_{3\times3} & \boldsymbol{P}_{\delta p^n} \end{bmatrix} \tag{4}$$

Where $\boldsymbol{P}_{\phi^n}$, $\boldsymbol{P}_{\delta v^n}$ and $\boldsymbol{P}_{\delta p^n}$ are the ECMs corresponding to $\boldsymbol{\phi}^n$, $\delta\boldsymbol{v}^n$ and $\delta\boldsymbol{p}^n$ respectively, and all three are diagonal matrices.

III. ECM OF SINS/GNSS BASED ON STEKF

The avp error states of SINS/GNSS based on STEKF could be defined as $\boldsymbol{X}_s = [(\boldsymbol{\phi}^n)^T \ (\delta\boldsymbol{v}_\phi^n)^T \ (\delta\boldsymbol{p}^n)^T]^T$, where $\delta\boldsymbol{v}_\phi^n$ is the transformed nonlinear velocity error, which can be described as [9]

$$\delta\boldsymbol{v}_\phi^n = \delta\boldsymbol{v}^n - (\tilde{\boldsymbol{v}}^n\times)\boldsymbol{\phi}^n \tag{5}$$

Where $\tilde{\boldsymbol{v}}^n$ is the estimated velocity, $(\bullet\times)$ represents the skew symmetric matrix operator. It can be seen from (5) that there is an extra term $-(\tilde{\boldsymbol{v}}^n\times)\boldsymbol{\phi}^n$ closely related to the misalignment angle in the new velocity error state, which results in strong correlation between the transformed error states. Therefore,

the new ECM should no longer be roughly initialized to a diagonal matrix.

The new error state $\boldsymbol{X}_s$ can be transformed from the traditional error state $\boldsymbol{X}_n$ as follows.

$$\boldsymbol{X}_s = \boldsymbol{A}_{sn}\boldsymbol{X}_n = \begin{bmatrix} \boldsymbol{I}_{3\times3} & 0_{3\times3} & 0_{3\times3} \\ -(\tilde{\boldsymbol{v}}^n\times) & \boldsymbol{I}_{3\times3} & 0_{3\times3} \\ 0_{3\times3} & 0_{3\times3} & \boldsymbol{I}_{3\times3} \end{bmatrix} \begin{bmatrix} \boldsymbol{\phi}^n \\ \boldsymbol{\delta v}^n \\ \boldsymbol{\delta p}^n \end{bmatrix} \tag{6}$$

The matrix $\boldsymbol{A}_{sn}$ represents the transformed relationship between error states $\boldsymbol{X}_s$ and $\boldsymbol{X}_n$, so it can be called the state transformation matrix. The system ECM after state transformation can be expressed as

$$\boldsymbol{P}_s = \mathrm{E}(\boldsymbol{X}_s\boldsymbol{X}_s^T) = \boldsymbol{A}_{sn}\mathrm{E}(\boldsymbol{X}_n\boldsymbol{X}_n^T)\boldsymbol{A}_{sn}^T = \boldsymbol{A}_{sn}\boldsymbol{P}_n\boldsymbol{A}_{sn}^T \tag{7}$$

It can be seen from (7) that the matrix $\boldsymbol{A}_{sn}$ also represents the transformed relationship between ECM $\boldsymbol{P}_s$ and $\boldsymbol{P}_n$. Substituting (4) and (6) into (7) as

$$\begin{aligned} \boldsymbol{P}_s = & \begin{bmatrix} \boldsymbol{I}_{3\times3} & 0_{3\times3} & 0_{3\times3} \\ -(\tilde{\boldsymbol{v}}^n\times) & \boldsymbol{I}_{3\times3} & 0_{3\times3} \\ 0_{3\times3} & 0_{3\times3} & \boldsymbol{I}_{3\times3} \end{bmatrix} \begin{bmatrix} \boldsymbol{P}_{\phi^n} & 0_{3\times3} & 0_{3\times3} \\ 0_{3\times3} & \boldsymbol{P}_{\delta v^n} & 0_{3\times3} \\ 0_{3\times3} & 0_{3\times3} & \boldsymbol{P}_{\delta p^n} \end{bmatrix} \cdots \\ & \begin{bmatrix} \boldsymbol{I}_{3\times3} & 0_{3\times3} & 0_{3\times3} \\ -(\tilde{\boldsymbol{v}}^n\times) & \boldsymbol{I}_{3\times3} & 0_{3\times3} \\ 0_{3\times3} & 0_{3\times3} & \boldsymbol{I}_{3\times3} \end{bmatrix}^T \\ = & \begin{bmatrix} \boldsymbol{P}_{\phi^n} & (\tilde{\boldsymbol{v}}^n\times)^T\boldsymbol{P}_{\phi^n} & 0_{3\times3} \\ \boldsymbol{P}_{\phi^n}(\tilde{\boldsymbol{v}}^n\times) & \boldsymbol{P}_{\delta v^n} + (\tilde{\boldsymbol{v}}^n\times)\boldsymbol{P}_{\phi^n}(\tilde{\boldsymbol{v}}^n\times)^T & 0_{3\times3} \\ 0_{3\times3} & 0_{3\times3} & \boldsymbol{P}_{\delta p^n} \end{bmatrix} \end{aligned} \tag{8}$$

As shown in (8), the ECM is obviously no longer a diagonal matrix and the elements on the diagonal have also changed, which verifies the analysis above.

IV. ECM OF SINS/GNSS BASED ON IEKF

IEKF can be divided into Right Invariant Kalman Filter (RIEKF) and Left Invariant Kalman Filter (LIEKF) due to different definition of error states [12]. In this section, the two kinds of ECM conversion models will be derived respectively.

A. ECM OF SINS/GNSS BASED ON RIEKF

he traditional error state can be described as $\boldsymbol{X}_e = [(\boldsymbol{\phi}^e)^T \ (\boldsymbol{\delta v}^e)^T \ (\boldsymbol{\delta r}^e)^T]^T$, where $\boldsymbol{\phi}^e$ is the attitude error (misalignment angle) of body frame with respect to Earth-Centered Earth-Fixed frame (ECEF). $\boldsymbol{\delta v}^e$ is the velocity error of body frame with respect to Earth Centered Inertial frame (ECI) represented in ECEF. $\boldsymbol{\delta r}^e$ is the Cartesian position error of body frame with respect to ECI represented in ECEF. The error state of RIEKF can be described as $\boldsymbol{X}_i^r = [(\boldsymbol{\phi}^e)^T \ (\boldsymbol{J\rho}_v^r)^T \ (\boldsymbol{J\rho}_r^r)^T]^T$, $\boldsymbol{J\rho}_v^r$ and $\boldsymbol{J\rho}_r^r$ are velocity error state and position error state redefined in Lie group, which can be described as [16]

$$\begin{aligned} \boldsymbol{J\rho}_v^r &= (\tilde{\boldsymbol{v}}^e\times)\boldsymbol{\phi}^e - \boldsymbol{\delta v}^e \\ \boldsymbol{J\rho}_r^r &= (\tilde{\boldsymbol{r}}^e\times)\boldsymbol{\phi}^e - \boldsymbol{\delta r}^e \end{aligned} \tag{9}$$

Where $\tilde{\boldsymbol{v}}^e$ and $\tilde{\boldsymbol{r}}^e$ are the estimated velocity and position respectively. It can be seen from (9) that there are extra terms $(\tilde{\boldsymbol{v}}^e\times)\boldsymbol{\phi}^e$ and $(\tilde{\boldsymbol{r}}^e\times)\boldsymbol{\phi}^e$, both related to the misalignment angle, which results in strong correlation between the transformed error states. Therefore, the new ECM of RIEKF should also not be roughly initialized to a diagonal matrix.

The RIEKF error state $\boldsymbol{X}_i^r$ can be transformed from the traditional error state $\boldsymbol{X}_e$ as follows.

$$\boldsymbol{X}_i^r = \boldsymbol{A}_{ir}\boldsymbol{X}_e = \begin{bmatrix} \boldsymbol{I}_{3\times3} & 0_{3\times3} & 0_{3\times3} \\ (\tilde{\boldsymbol{v}}^e\times) & -\boldsymbol{I}_{3\times3} & 0_{3\times3} \\ (\tilde{\boldsymbol{r}}^e\times) & 0_{3\times3} & -\boldsymbol{I}_{3\times3} \end{bmatrix} \begin{bmatrix} \boldsymbol{\phi}^e \\ \boldsymbol{\delta v}^e \\ \delta\boldsymbol{r}^e \end{bmatrix} \tag{10}$$

The matrix $\boldsymbol{A}_{ir}$ also represents the transformed relationship between error states $\boldsymbol{X}_i^r$ and $\boldsymbol{X}_e$. The system ECM after state transformation can be expressed as

$$\boldsymbol{P}_i^r = \mathrm{E}[\boldsymbol{X}_i^r(\boldsymbol{X}_i^r)^T] = \boldsymbol{A}_{ir}\mathrm{E}(\boldsymbol{X}_e\boldsymbol{X}_e^T)\boldsymbol{A}_{ir}^T = \boldsymbol{A}_{ir}\boldsymbol{P}_e\boldsymbol{A}_{ir}^T \tag{11}$$

Where $\boldsymbol{P}_e$ is the ECM corresponding to the traditional error state $\boldsymbol{X}_e$, and its derivation process is the same as that of $\boldsymbol{P}_n$. Let

$$\boldsymbol{P}_e = \mathrm{E}(\boldsymbol{X}_e\boldsymbol{X}_e^T) = \begin{bmatrix} \boldsymbol{P}_{\phi^e} & 0_{3\times3} & 0_{3\times3} \\ 0_{3\times3} & \boldsymbol{P}_{\delta v^e} & 0_{3\times3} \\ 0_{3\times3} & 0_{3\times3} & \boldsymbol{P}_{\delta r^e} \end{bmatrix} \tag{12}$$

Where $\boldsymbol{P}_{\phi^e}$, $\boldsymbol{P}_{\delta v^e}$ and $\boldsymbol{P}_{\delta r^e}$ are the ECMs corresponding to $\boldsymbol{\phi}^e$, $\boldsymbol{\delta v}^e$ and $\boldsymbol{\delta r}^e$ respectively, and all three are diagonal matrices. It can be seen from (11) that the matrix $\boldsymbol{A}_{ir}$ also represents the transformed relationship between ECM $\boldsymbol{P}_i^r$ and $\boldsymbol{P}_e$. Substituting (10) and (12) into (11) as

$$\boldsymbol{P}_i^r = \begin{bmatrix} \boldsymbol{I}_{3\times3} & 0_{3\times3} & 0_{3\times3} \\ (\tilde{\boldsymbol{v}}^e\times) & -\boldsymbol{I}_{3\times3} & 0_{3\times3} \\ (\tilde{\boldsymbol{r}}^e\times) & 0_{3\times3} & -\boldsymbol{I}_{3\times3} \end{bmatrix} \begin{bmatrix} \boldsymbol{P}_{\phi^e} & 0_{3\times3} & 0_{3\times3} \\ 0_{3\times3} & \boldsymbol{P}_{\delta v^e} & 0_{3\times3} \\ 0_{3\times3} & 0_{3\times3} & \boldsymbol{P}_{\delta r^e} \end{bmatrix} \cdots$$

$$\begin{bmatrix} \boldsymbol{I}_{3\times3} & 0_{3\times3} & 0_{3\times3} \\ (\tilde{\boldsymbol{v}}^e\times) & -\boldsymbol{I}_{3\times3} & 0_{3\times3} \\ (\tilde{\boldsymbol{r}}^e\times) & 0_{3\times3} & -\boldsymbol{I}_{3\times3} \end{bmatrix}^T =$$

$$\begin{bmatrix} \boldsymbol{P}_{\phi^e} & \boldsymbol{P}_{\phi^e}(\tilde{\boldsymbol{v}}^e\times)^T & \boldsymbol{P}_{\phi^e}(\tilde{\boldsymbol{r}}^e\times)^T \\ (\tilde{\boldsymbol{v}}^e\times)\boldsymbol{P}_{\phi^e} & \boldsymbol{P}_{\delta v^e} + (\tilde{\boldsymbol{v}}^e\times)\boldsymbol{P}_{\phi^e}(\tilde{\boldsymbol{v}}^e\times)^T & (\tilde{\boldsymbol{v}}^e\times)\boldsymbol{P}_{\phi^e}(\tilde{\boldsymbol{r}}^e\times)^T \\ (\tilde{\boldsymbol{r}}^e\times)\boldsymbol{P}_{\phi^e} & (\tilde{\boldsymbol{r}}^e\times)\boldsymbol{P}_{\phi}(\tilde{\boldsymbol{v}}^e\times)^T & \boldsymbol{P}_{\delta r^e} + (\tilde{\boldsymbol{r}}^e\times)\boldsymbol{P}_{\phi^e}(\tilde{\boldsymbol{r}}^e\times)^T \end{bmatrix} \tag{13}$$

As shown in (13), the ECM is obviously also not a diagonal matrix and the elements on the diagonal have changed, which verifies the analysis above.

B. ECM OF SINS/GNSS BASED ON LIEKF

The error state of LIEKF can be described as $\boldsymbol{X}_i^l = [(\boldsymbol{\phi}^b)^T \ (\boldsymbol{J}\boldsymbol{\rho}_v^l)^T \ (\boldsymbol{J}\boldsymbol{\rho}_r^l)^T]^T$, $\boldsymbol{J}\boldsymbol{\rho}_v^l$ and $\boldsymbol{J}\boldsymbol{\rho}_r^l$ are velocity error state and position error state redefined in Lie group, which can be described as [16]

$$\begin{aligned} \boldsymbol{\phi}^b &= \tilde{\boldsymbol{C}}_e^b\boldsymbol{\phi}^e \\ \boldsymbol{J}\boldsymbol{\rho}_v^l &= -\tilde{\boldsymbol{C}}_e^b\delta\boldsymbol{v}^e \\ \boldsymbol{J}\boldsymbol{\rho}_r^l &= -\tilde{\boldsymbol{C}}_e^b\delta\boldsymbol{r}^e \end{aligned} \tag{14}$$

The LIEKF error state $\boldsymbol{X}_i^l$ can be transformed from the traditional error state $\boldsymbol{X}_e$ as follows.

$$\boldsymbol{X}_i^l = \boldsymbol{A}_{il}\boldsymbol{X}_e = \begin{bmatrix} \tilde{\boldsymbol{C}}_e^b & 0_{3\times3} & 0_{3\times3} \\ 0_{3\times3} & -\tilde{\boldsymbol{C}}_e^b & 0_{3\times3} \\ 0_{3\times3} & 0_{3\times3} & -\tilde{\boldsymbol{C}}_e^b \end{bmatrix} \begin{bmatrix} \boldsymbol{\phi}^e \\ \delta\boldsymbol{v}^e \\ \delta\boldsymbol{r}^e \end{bmatrix} \tag{15}$$

The matrix $\boldsymbol{A}_{il}$ represents the transformed relationship between error states $\boldsymbol{X}_i^l$ and $\boldsymbol{X}_e$. The system ECM after state transformation can be expressed as

$$\boldsymbol{P}_i^l = \mathrm{E}[\boldsymbol{X}_i^l(\boldsymbol{X}_i^l)^T] = \boldsymbol{A}_{il}\mathrm{E}(\boldsymbol{X}_e\boldsymbol{X}_e^T)\boldsymbol{A}_{il}^T = \boldsymbol{A}_{il}\boldsymbol{P}_e\boldsymbol{A}_{il}^T \tag{16}$$

It can be seen from (16) that the matrix $\boldsymbol{A}_{il}$ also represents the transformed relationship between ECM $\boldsymbol{P}_i^l$ and $\boldsymbol{P}_e$. Substituting (12) and (15) into (16) as

$$\boldsymbol{P}_i^l = \begin{bmatrix} \tilde{\boldsymbol{C}}_e^b & 0_{3\times3} & 0_{3\times3} \\ 0_{3\times3} & -\tilde{\boldsymbol{C}}_e^b & 0_{3\times3} \\ 0_{3\times3} & 0_{3\times3} & -\tilde{\boldsymbol{C}}_e^b \end{bmatrix} \begin{bmatrix} \boldsymbol{P}_{\phi^e} & 0_{3\times3} & 0_{3\times3} \\ 0_{3\times3} & \boldsymbol{P}_{\delta v^e} & 0_{3\times3} \\ 0_{3\times3} & 0_{3\times3} & \boldsymbol{P}_{\delta r^e} \end{bmatrix} \cdots$$

$$\begin{bmatrix} \tilde{\boldsymbol{C}}_e^b & 0_{3\times3} & 0_{3\times3} \\ 0_{3\times3} & -\tilde{\boldsymbol{C}}_e^b & 0_{3\times3} \\ 0_{3\times3} & 0_{3\times3} & -\tilde{\boldsymbol{C}}_e^b \end{bmatrix}^T = \tag{17}$$

$$\begin{bmatrix} \tilde{\boldsymbol{C}}_e^b\boldsymbol{P}_{\phi^e}(\tilde{\boldsymbol{C}}_e^b)^T & 0_{3\times3} & 0_{3\times3} \\ 0_{3\times3} & \tilde{\boldsymbol{C}}_e^b\boldsymbol{P}_{\delta v^e}(\tilde{\boldsymbol{C}}_e^b)^T & 0_{3\times3} \\ 0_{3\times3} & 0_{3\times3} & \tilde{\boldsymbol{C}}_e^b\boldsymbol{P}_{\delta r^e}(\tilde{\boldsymbol{C}}_e^b)^T \end{bmatrix}$$

As shown in (17), $\tilde{\boldsymbol{C}}_e^b\boldsymbol{P}_{\phi^e}(\tilde{\boldsymbol{C}}_e^b)^T$, $\tilde{\boldsymbol{C}}_e^b\boldsymbol{P}_{\delta v^e}(\tilde{\boldsymbol{C}}_e^b)^T$ and $\tilde{\boldsymbol{C}}_e^b\boldsymbol{P}_{\delta r^e}(\tilde{\boldsymbol{C}}_e^b)^T$ are usually no longer diagonal matrices, although $\boldsymbol{P}_{\phi^e}$, $\boldsymbol{P}_{\delta v^e}$ and $\boldsymbol{P}_{\delta r^e}$ are all diagonal matrices. In fact, the attitude, velocity and position error stats of LIEKF are still not correlated, but after the transformation as shown in (14), the three-dimensional components of each error state may be correlated. Therefore, it is not accurate to initialize the ECM with a diagonal matrix.

V. EXPERIMENT RESULTS AND DISCUSSION

A set of shipborne SINS/GPS measurements was adopt to verify the effectiveness of the ECM initialization method proposed in this paper. The experimental platform and equipment are shown in Fig. 1.

FIGURE 1. Equipment of boat-mounted field experiment.

The experimental equipment related to this paper includes one SINS and two GPS systems. One GPS worked in real-time kinematic (RTK) mode with SINS to constitute an integrated navigation system to provide high-precision navigation reference information, the other worked in precise point positioning (PPP) mode to provide position

measurements. The main parameters of experimental sensors are shown in Table I.

TABLE I
MAIN PARAMETERS OF EXPERIMENTAL SENSORS.

Sensors	Index	Parameter
SINS	Gyro drift	$0.003°/h$
	Gyro random noise	$0.0005°/\sqrt{h}$
	Accelerometer bias	$[40,30,90]$ ug
	Accelerometer noise	$[10,10,20]$ ug$/\sqrt{\text{Hz}}$
	Data update rate	200Hz
GPS	Measurement accuracy	0.1m
	Data update rate	1Hz

The total duration of the experiment was 12600s, the experimental ship was in a static state in the first 1000s, mainly for the initial alignment and calibration of experimental equipment. After that, a series of smooth maneuvers and variable velocity maneuvers were carried out to meet a variety of experimental requirements. In this paper, the measured data of SINS/GPS integrated system between 2000s-3000s were selected for experimental verification. The movement trajectory of experimental ship was shown in Fig. 2.

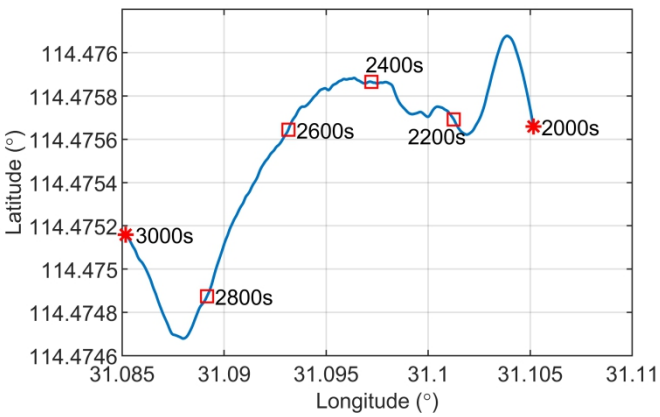

FIGURE 2. Trajectory of experimental ship.

Remark 1. SINS/GNSS integrated navigation models based on STEKF and IEKF have been been introduced in detail in reference [9,16], which are not discussed in this paper.

Remark 2. Yaw Error and Horizontal-position Error (Hori-Error) are the key technical indexes of SINS/GPS integrated system, which can reflect the performance of different algorithms directly. Therefore, these two parameters are selected to verify the effect of ECM initialization based on error states correlation.

Remark 3. Since STEKF and IEKF have more significant advantages in the case of large misalignment angle, the variances of initial misalignment angle, velocity error and position error are respectively set as $[5°,5°,50°]^2$, $[0.1\text{m/s},0.1\text{m/s},0.1\text{m/s}]^2$, $[1\text{m},1\text{m},1\text{m}]^2$, which are all represented in ENU navigation frame.

A. SINS/GNSS EXPERIMENT BASED ON STEKF

As shown in Fig. 3, in the case of ECM $\boldsymbol{P}$ initialized based on error state correlation (hereinafter referred to as $\boldsymbol{P}_{ibc}$, which is described as " $\boldsymbol{P}$ initialized by correlation" in figures), the yaw error of STEKF has rapidly converged to within 1° before 120s, which is significantly better than that of ECM $\boldsymbol{P}$ initialized based on diagonal matrix (hereinafter referred to as $\boldsymbol{P}_{ibd}$, which is described as " $\boldsymbol{P}$ initialized by diagonalization" in figures). As can be seen from Fig. 4, after STEKF is started, the Hori-Error of $\boldsymbol{P}_{ibc}$ immediately converges to less than 0.5m, while that of $\boldsymbol{P}_{ibd}$ gradually converges to less than 1m after 200s, and there are relatively large oscillations.

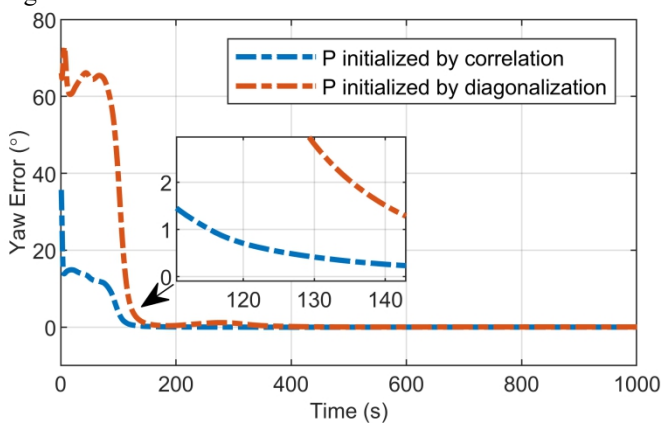

FIGURE 3. Yaw errors based on STEKF for $\boldsymbol{P}_{ibc}$ and $\boldsymbol{P}_{ibd}$.

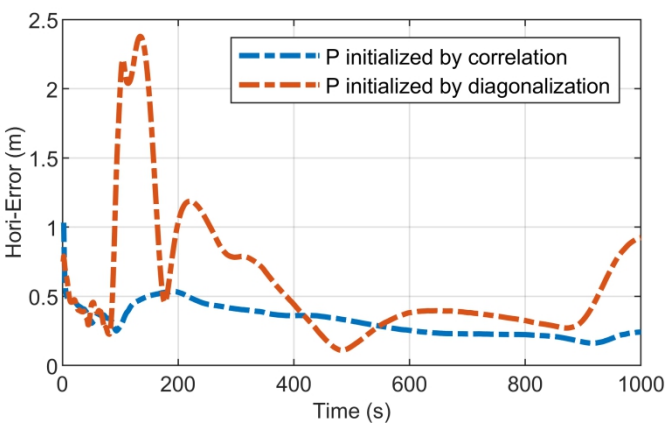

FIGURE 4. Hori-Errors based on STEKF for $\boldsymbol{P}_{ibc}$ and $\boldsymbol{P}_{ibd}$.

In order to visually compare the influence of the two methods on the accuracy of error state estimation, the Root Mean Square Error (RMSE) was calculated since the error curves were basically stable at 200s (followings are the same). It can be seen from Table II that the convergence accuracy of yaw error and Hori-Error based on $\boldsymbol{P}_{ibc}$ also obviously performed better than that based on $\boldsymbol{P}_{ibd}$.

TABLE II
RMSEs OF YAW ERROR AND HORI-ERROR BASED ON STEKF FOR $\boldsymbol{P}_{ibc}$ AND $\boldsymbol{P}_{ibd}$.

Methods	Yaw Error (°)	Hori-Error (m)
$\boldsymbol{P}_{ibc}$	0.012	0.31
$\boldsymbol{P}_{ibd}$	0.384	0.56

TABLE III
RMSEs OF YAW ERROR AND HORI-ERROR BASED ON RIEKF FOR $\boldsymbol{P}_{ibc}$ AND $\boldsymbol{P}_{ibd}$.

Methods	Yaw Error (°)	Hori-Error (m)
$\boldsymbol{P}_{ibc}$	0.272	0.33
$\boldsymbol{P}_{ibd}$	0.692	2.90

B. SINS/GNSS EXPERIMENT BASED ON RIEKF

As shown in Fig. 5, the yaw error of $\boldsymbol{P}_{ibc}$ based on RIEKF has rapidly converged to within 2° around 120s, which is significantly faster than the convergence speed of $\boldsymbol{P}_{ibd}$. As can be seen from Fig. 6, after RIEKF is started, the Hori-Error of $\boldsymbol{P}_{ibc}$ immediately converges to within 2m, while that of $\boldsymbol{P}_{ibd}$ only converges to around 5m after 200s, and there are relatively large oscillations.

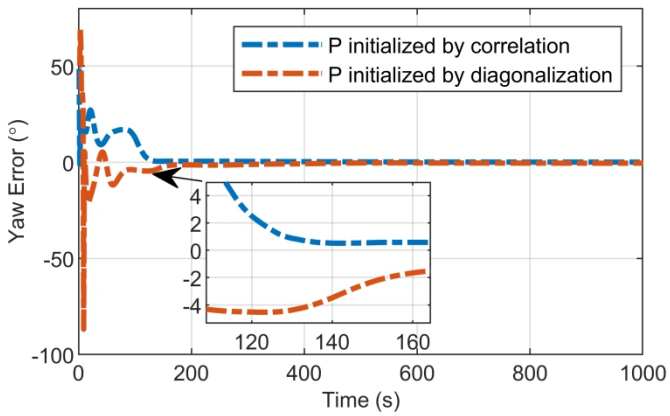

FIGURE 5. Yaw errors based on RIEKF for $\boldsymbol{P}_{ibc}$ and $\boldsymbol{P}_{ibd}$.

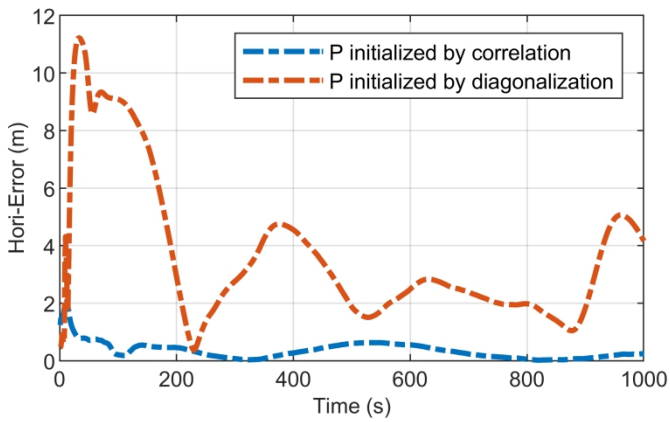

FIGURE 6. Hori-Errors based on RIEKF for $\boldsymbol{P}_{ibc}$ and $\boldsymbol{P}_{ibd}$.

It can be seen from Table III that the convergence accuracy of yaw error and Hori-Error based on $\boldsymbol{P}_{ibc}$ also obviously performed better than that based on $\boldsymbol{P}_{ibd}$.

C. SINS/GNSS EXPERIMENT BASED ON LIEKF

As shown in Fig. 7, the yaw error of $\boldsymbol{P}_{ibc}$ based on LIEKF has rapidly converged to within 1° around 90s, which is significantly faster than the convergence speed of $\boldsymbol{P}_{ibd}$. As can be seen from Fig. 8, after RIEKF is started, the Hori-Error of $\boldsymbol{P}_{ibc}$ immediately converges to within 0.6m, while that of $\boldsymbol{P}_{ibd}$ only converges to within 0.6m after 100s.

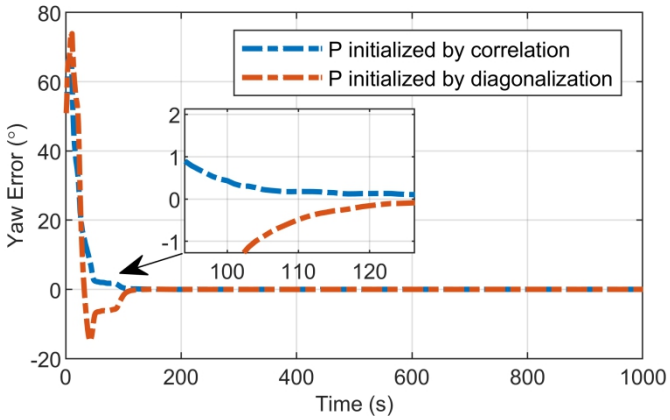

FIGURE 7. Yaw errors based on LIEKF for $\boldsymbol{P}_{ibc}$ and $\boldsymbol{P}_{ibd}$.

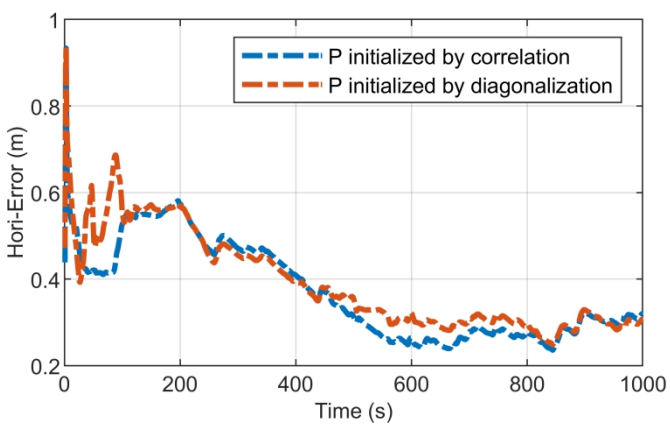

FIGURE 8. Hori-Errors based on LIEKF for $\boldsymbol{P}_{ibc}$ and $\boldsymbol{P}_{ibd}$.

As shown in Table IV, the convergence accuracy of yaw error based on $\boldsymbol{P}_{ibc}$ is about 0.008° better than that based on $\boldsymbol{P}_{ibd}$, the convergence accuracy of Hori-Error based on $\boldsymbol{P}_{ibc}$ is about 0.01m better than that based on $\boldsymbol{P}_{ibd}$. It can be

found that the performance advantage of $\boldsymbol{P}_{ibc}$ over $\boldsymbol{P}_{ibd}$ in LIEKF is less significant than that in STEKF and RIEKF. According to the analysis in chapter 4.2, this is because the attitude, velocity and position error of LIEKF are not correlated with each other, and the correlation only exists between the three-dimensional components of each error state, however, $\boldsymbol{P}_{ibc}$ still showed better performance.

TABLE IV
RMSEs of Yaw Error and Hori-Error Based on LIEKF for $\boldsymbol{P}_{ibc}$ and $\boldsymbol{P}_{ibd}$.

Methods	Yaw Error (°)	Hori-Error (m)
$\boldsymbol{P}_{ibc}$	0.005	0.35
$\boldsymbol{P}_{ibd}$	0.013	0.36

VI. CONCLUSIONS

The ECM initialization method based on the correlation of nonlinear error states is proposed in this paper. The theoretical basis for the ECM initialization of STEKF and IEKF is first established through the derivation and analysis of the transformed models for ECM. Then the shipborne SINS/GNSS experiment is carried out, and the results show that the proposed method has better performance in SINS/GNSS states estimation than traditional method. In addition, the ECM initialization based on error states correlation can also be applied to SINS/DVL, SINS/CNS and other integrated systems, as well as other optimal estimation algorithms involving transformed states.

REFERENCES

[1] Sun, J.; Chen, Z.; Wang, F. A Novel ML-Aided Methodology for SINS/GPS Integrated Navigation Systems during GPS Outages. Remote Sensing, vol. 14, no. 23, pp. 5932, 2022.
[2] Liao, M.; Liu, J.; Meng, Z.; You, Z. A SINS/SAR/GPS Fusion Positioning System Based on Sensor Credibility Evaluations. Remote Sensing, vol. 13, no. 21, pp. 4463, 2021.
[3] Wendel, J.; Maier, A.; Metzger, J. and Trommer, G. F. Comparison of Extended and Sigma-Point Kalman Filters for Tightly Coupled GPS/INS Integration. presented at AIAA guidance, navigation, and control Conf. and exhibit, San Francisco, California, USA, Aug. 15-18, 2005.
[4] Nasser, E. et al. Analysis of Various Kalman Filter Algorithms Using Different Inertial Navigation Systems Integrated with the Global Positioning System. Canadian Aeronautics and Space Journal, vol. 52, no. 2, pp. 59-67, June 2006.
[5] Gross, J. et al. A Comparison of Extended Kalman Filter, Sigma-Point Kalman Filter, and Particle Filter in GPS/INS Sensor Fusion. presented at AIAA guidance, navigation, and control Conf., Toronto, Ontario, Canada, Aug. 2-5, 2010.
[6] Zhang, X.; Zhu, F.; Tao, X. and Duan, R. New Optimal Smoothing Scheme for Improving Relative and Absolute Accuracy of Tightly Coupled GNSS/SINS Integration. GPS Solutions, vol. 21, pp. 861-872, Jan. 2017.
[7] Chang, L.; Bian, Q.; Zuo, Y. and Zhou, Q. SINS/GNSS Integrated Navigation Based on Group Affine SINS Mechanization in Local-Level Frame. in IEEE/ASME Transactions on Mechatronics, doi: 10.1109/TMECH.2023.3252044.
[8] Du, S.; Huang, Y.; Lin, B.; Qian, J. and Zhang, Y. A Lie Group Manifold-Based Nonlinear Estimation Algorithm and Its Application to Low-Accuracy SINS/GNSS Integrated Navigation. in IEEE Transactions on Instrumentation and Measurement, vol. 71, pp. 1-27, 2022, Art no. 1002927, doi: 10.1109/TIM.2022.3159950.
[9] Wang, M. et al. State Transformation Extended Kalman Filter for GPS/SINS Tightly Coupled Integration. GPS Solutions, vol. 22, pp. 1-12, Aug. 2018.
[10] Wang, M.; Cui, J.; Huang, Y.; Wu, W. and Du, X. Schmidt ST-EKF for Autonomous Land Vehicle SINS/ODO/LDV Integrated Navigation. IEEE Trans. Instrum. Meas., vol. 70, pp. 1-9, 2021.
[11] Wang, M.; Wu, W.; He, X.; Li, Y. and Pan, X. Pan. Consistent ST-EKF for Long Distance Land Vehicle Navigation Based on SINS/OD Integration. IEEE Trans. Veh. Technol., vol. 68, no. 11, pp. 10525-10534, 2019.
[12] Barrau,A.; Bonnabel, S. The Invariant Extended Kalman Filter as a Stable Observer. IEEE Transaction on Automatic Control, vol. 62, no. 4, pp. 1797-1812, 2017.
[13] Barrau,A.; Bonnabel, S. Intrinsic Filtering on Lie Groups with Applications to Attitude Estimation. IEEE Transactions on Automatic Control, vol. 60, no. 2, pp. 436–449, 2015.
[14] Ross, H. et al. Contact-Aided Invariant Extended Kalman Filtering for Robot State Estimation. The International Journal of Robotics Research, vol. 39, no. 4, pp. 402-430, Jan. 2020.
[15] Emmanuel, R.; Perrot, T. Invariant Filtering Versus Other Robust Filtering Methods Applied to Integrated Navigation. presented at 2017 24th Saint Petersburg International Conf. on Integrated Navigation Systems (ICINS), St. Petersburg, Russia, May 29-31, 2017.
[16] Luo, Y.; Guo, C.; You, S.; Hu, J. and Liu, J. SE2(3) Based Extended Kalman Filtering and Smoothing Framework for Inertial-Integrated Navigation. Available: http://arxiv.org/abs/2102.12897, 2021.
[17] Hartley, R.; Ghaffari, M.; Eustice, R. M. and Grizzle, J. W. Contact-Aided Invariant Extended Kalman Filtering for Robot State Estimation. The International Journal of Robotics Research, vol. 39, no. 4, pp. 402-430, 2020.
[18] Barrau,A.; Bonnabel, S. Invariant Kalman Filtering. Annu. Rev. Control, Robot. Auton. Syst., vol. 1, pp. 237–257, May 2018.
[19] Barrau,A. Non-Linear State Error Based Extended Kalman Filters with Applications to Navigation. Ph.D. dissertation, Mines Paristech, 2015.
[20] Groves, P. D. Principles of GNSS, Inertial, and Multisensor Integrated Navigation Systems. Norwood, MA, USA, 2008.
[21] Cui, J. et al. Lie Group Based Nonlinear State Errors for MEMS-IMU/GNSS/Magnetometer Integrated Navigation. The Journal of Navigation, vol. 74, no. 4, pp. 887-900, 2021.
[22] Tang, H. et al. Invariant Error-Based Integrated Solution for SINS/DVL in Earth Frame: extension and comparison. IEEE Transactions on Instrumentation and Measurement, vol. 72, 2022, doi: 10.1109/TIM.2022.3225043.
[23] Luo, L.; Huang, Y.; Zhang, Z. et al. A New Kalman Filter-Based In-Motion Initial Alignment Method for DVL-Aided Low-Cost SINS. IEEE Transactions on Vehicular Technology, vol. 70, no. 1, pp. 331-343, 2021.
[24] Tang, J.; Bian, H.; Ma, H. et al. One-Step Initial Alignment Algorithm for SINS in the ECI Frame Based on the Inertial Attitude Measurement of the CNS. Sensors, vol. 22, no. 14. pp. 5123, 2022.
[25] Lu, Y. Study of CNS/INS Integrated Navigation System Based on Speed Damping Technology. Optics & Optoelectronic Technology, vol. 10, no. 04. pp. 62-67, 2012.

Jun Tang was born in Dalian, China, Feb. 1983. He received the B.Sc. degree in ship navigation from Dalian Naval Academy, Dalian, China, in 2006 and the M.Sc. degree in traffic information engineering and control from Dalian Naval Academy, Dalian, China, in 2011. He is currently pursuing the Ph.D. degree in navigation, guidance, and control with Naval University of Engineering, Wuhan, China. His research interests include inertial navigation, celestial navigation and integrated navigation.

Hongwei Bian received the M.S. degree in navigation, guidance and control from the Naval University of Engineering, Wuhan, China, in 1997 and the Ph.D. degree in instrument science and engineering from Shanghai Jiao Tong University, Shanghai, China, in 2005. He is currently working as a Professor with the Naval University of Engineering. His current research interests include position navigation and timing, inertial navigation, integrated navigation theory, and information fusion.

Heng Ma received the M.S. degree in navigation, guidance and control from the Naval University of Engineering, Wuhan, China, in 2003 and the Ph.D. degree in electrical system and automation from Naval University of Engineering, Wuhan, China, in 2008. He is currently working as a Lecturer with the Naval University of Engineering. His current research interests include inertial navigation technology.

Rongying Wang received the Ph.D. degree in navigation, guidance and control from the Naval University of Engineering, Wuhan, China, in 2011. He is currently working as a Lecturer with the Naval University of Engineering. His current research interests include inertial navigation and integrated navigation.